AGU PUBLICATIONS

JGR

Journal of Geophysical Research: Solid Earth

RESEARCH ARTICLE
10.1002/2015JB012218

Key Points:
- A rapid estimation of runup is obtained based on finite fault models and centroid moment tensor
- Fast analytical methods to estimate near-field runup
- Useful for tsunami early warning purposes

Correspondence to:
S. Riquelme,
sebastian@dgf.uchile.cl

Citation:
Riquelme, S., M. Fuentes, G. P. Hayes, and J. Campos (2015), A rapid estimation of near-field tsunami runup, *J. Geophys. Res. Solid Earth*, *120*, 6487–6500, doi:10.1002/2015JB012218.

Received 20 MAY 2015
Accepted 10 AUG 2015
Accepted article online 19 AUG 2015
Published online 26 SEP 2015

A rapid estimation of near-field tsunami runup

Sebastián Riquelme[1], Mauricio Fuentes[2], Gavin P. Hayes[3], and Jaime Campos[2]

[1]National Seismological Center, University of Chile, Santiago, Chile, [2]Department of Geophysics, University of Chile, Santiago, Chile, [3]National Earthquake Information Center, United States Geological Survey, Golden, Colorado, USA

Abstract Many efforts have been made to quickly estimate the maximum runup height of tsunamis associated with large earthquakes. This is a difficult task because of the time it takes to construct an accurate tsunami model using real-time data from the source. It is possible to construct a database of potential seismic sources and their corresponding tsunami a priori. However, such models are generally based on uniform slip distributions and thus oversimplify the knowledge of the earthquake source. Here we show how to predict tsunami runup from any seismic source model using an analytic solution that is specifically designed for subduction zones with a well-defined geometry, i.e., Chile, Japan, Nicaragua, and Alaska. The main idea of this work is to provide a tool for emergency response, trading off accuracy for speed. The solutions we present for large earthquakes appear promising. Here runup models are computed for the following: the 1992 M_w 7.7 Nicaragua earthquake, the 2001 M_w 8.4 Perú earthquake, the 2003 M_w 8.3 Hokkaido earthquake, the 2007 M_w 8.1 Perú earthquake, the 2010 M_w 8.8 Maule earthquake, the 2011 M_w 9.0 Tohoku earthquake, and the recent 2014 M_w 8.2 Iquique earthquake. The maximum runup estimations are consistent with measurements made inland after each event, with a peak of 9 m for Nicaragua, 8 m for Perú (2001), 32 m for Maule, 41 m for Tohoku, and 4.1 m for Iquique. Considering recent advances made in the analysis of real-time GPS data and the ability to rapidly resolve the finiteness of a large earthquake close to existing GPS networks, it will be possible in the near future to perform these calculations within the first minutes after the occurrence of similar events. Thus, such calculations will provide faster runup information than is available from existing uniform-slip seismic source databases or past events of premodeled seismic sources.

1. Introduction

The maximum water height reached inland (runup) is an important geophysical parameter to characterize after a tsunami. It can be used to quantify how much damage a tsunami will generate in a given region (fatalities, economic losses [*Borrero et al.*, 2005], impact on critical operations, and facilities). Real-time runup and horizontal inundation prediction, if accurate, are powerful tools for government, decision makers and operational managers of communities, critical facilities, and cities.

The amplitude of the initial waves and its consequent runup is controlled by dip angle, strike, fault length, fault slip, mechanism, and proximity to the seafloor [*Ward*, 1980, 2011]. The dip and rake angles of the mechanism are related to the displacement that the source causes on the seafloor. Strike controls the directivity of the wave and its consequent amplification in the strike direction; when strike is parallel to the coast, tsunami waves will reach their maximum potential runup, while the minimum potential runup will occur when the strike is perpendicular to the shoreline [*Fuentes et al.*, 2013]. In the near field, the area affected by the runup is related to the fault extension [*Okal and Synolakis*, 2004], and in turn the proximity of the upper part of the fault to the seafloor controls how much displacement is transferred from the subsurface into the water column [*Okada*, 1985]. In the case of a shallow fault dip, significant inelastic seafloor uplift can occur, resulting in increased the deformation, while the largest uplift would be located landward from the trench, amplifying the runup [*Ma*, 2012]. Knowledge of these parameters provides enough information to estimate the tsunamigenic potential. However, these parameters alone do not allow for quantification of runup along the coast.

Tsunami early warning systems quantify the tsunamigenic potential of any earthquake. Various approaches based on seismic and/or geodetic data make it possible to estimate moment magnitude and mechanism [*Kanamori and Rivera*, 2008; *Blewitt et al.*, 2009; *Lomax and Michelini*, 2009, 2011]. Using scaling laws

[*Wells and Coppersmith*, 1994; *Blaser et al.*, 2010; *Strasser et al.*, 2010; *Murotani et al.*, 2013], one can obtain empirical estimates of rupture length, width, and average slip and then take the best tsunami model (from a large, precomputed database) that fits accurately with the estimated characteristics of the earthquake. Nevertheless, these tsunami models do not include variable slip in the source, which can cause large uncertainties in runup prediction. *Reymond et al.* [2012], on the basis of a precomputed data set of 260 scenarios, developed a forecasting tool to estimate tsunami amplitudes, both on the high seas and in targeted coastal areas in French Polynesia. This method takes just 1 min to calculate those amplitudes. However, it does not work well enough, as the author explains, at specific locations because some parameters associated to Green's Law need to be calibrated.

From the seismological point of view, realistic seismic sources need to be considered. These sources respect the earthquake physics. They include properties associated to fractal laws, spectral decay, and nonuniform slip [*Andrews*, 1980, 1981; *Herrero and Bernard*, 1994; *Bernard et al.*, 1996] which are more accurately accounted for in distributed slip fault models than on a fault plane with constant slip. Using an approach that incorporates realistic seismic sources, *Geist* [2002] showed that earthquakes modeled with uniform slip can underestimate the runup, up to 6 times in comparison with runup calculated with nonuniform slip in the near field. Recent studies in New Zealand [*Mueller et al.*, 2015] and Chile [*Ruiz et al.*, 2015] support this conclusion. Thus, from these approaches we extract the idea of including complexity in our methods, i.e., finite fault models (FFM).

Some efforts have been made to obtain the slip distribution and runup in real time with near-field data. *Ohta et al.* [2012] used Real-Time Kinematic-GPS technology to obtain a fault model, which in theory could have been calculated in 4 min and 35 s. Another way to calculate the slip distribution of an earthquake is to use, Precise Point Position (PPP) of raw GPS data [*Hoechner et al.*, 2013]. By using strong motion, GPS, pressure sensors, and GPS buoys, combined, it is possible to more accurately model the slip distribution of the earthquake [*Melgar and Bock*, 2015]. *Hoechner et al.* [2013], and *Melgar and Bock* [2015], authors mentioned they calculated the runup with a full numerical model using a FFM as an initial condition.

Another approach is to use hydrodynamic inversion for tsunami forecasting. This can be done from unit sources in a very short time [*Titov et al.*, 2011]. Taking the data from Deep-Ocean Assessment and Reporting of Tsunamis (DART) buoys to constrain the source, using a precomputed unit slip source to derive associated deformation via Okada's equations, one can generate the initial condition to propagate tsunami. For the 2011 Japan tsunami it was possible to constrain the source using two DART buoys recording the first wave [*Tang et al.*, 2012] then propagate the theoretical tsunami and obtain accurate results at 28 tsunami meters throughout the Pacific.

Here we propose two new rapid methods to estimate near-field runup along the coastline: the first is based on using finite fault models in combination with a simple bathymetry model to estimate a rapid first-order approximation of 2+1 D tsunami runup distribution associated with any ocean deformation. The second approach is based on using the centroid moment tensor (CMT), which allows us to estimate an average seafloor uplift in order to approximate the maximum runup using a 1+1 D multisloping beach approach. These new tools will facilitate the computation of rapid and accurate run-up estimates and can be applied as soon as seismic characterization is complete.

2. Method

The problem of runup estimation has been broadly studied; in particular, *Okal and Synolakis* [2004] propose an empirical formula for the runup ($\mathcal{R}$) distribution along the coastline coordinate (y) for a simple uniform dislocation,

$$\mathcal{R}(y) = \frac{b}{1 + \left(\frac{y-c}{a}\right)^2} \tag{1}$$

where a, b, c are parameters determined by trial and error to fit the observed data (Figure 1). The authors propose that the aspect ratio $I_2 = b/a$ can be used as a discriminant of the tsunami source. They conclude that tsunamis associated with seismic sources have I_2 smaller than 10^{-4}, whereas landslide sources have larger values.

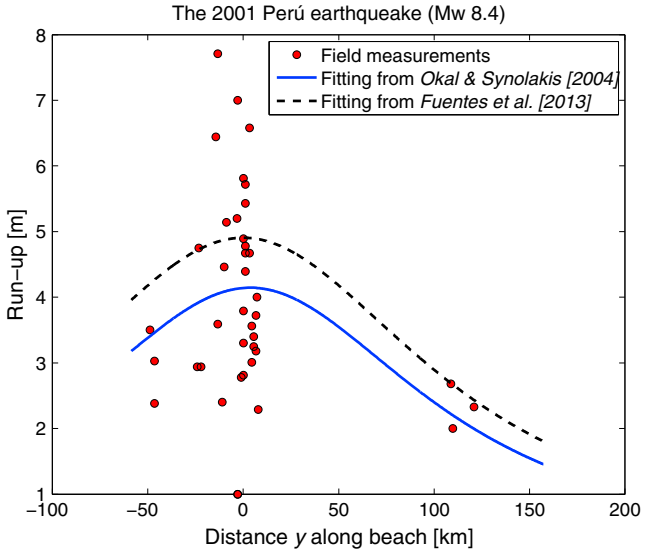

Figure 1. Validation of the analytical solution obtained by *Fuentes et al.* [2013].

The method proposed here is based on the formula of *Fuentes et al.* [2013] as an extension of *Synolakis* [1987]:

$$\begin{aligned} \mathcal{R}(y) &= f(p_0)\mathcal{R}_0\sqrt{\sin(\theta)} \\ \mathcal{R}_0 &= 2.831H\left(\frac{H}{d}\right)^{1/4}\sqrt{\alpha\cot(\beta)} \\ p_0 &= \alpha y\sin(\theta) - (x_1 - x_0)\cos(\theta) \\ \alpha &= \sqrt{1+\frac{H}{d}} \end{aligned} \tag{2}$$

Equation (2) includes a decay function along the transverse direction, which allows us to represent waves of bounded size. Choosing $f(p) = 1/\left[1+\left(\frac{2p}{L}\right)^2\right]$, a Lorenzian function, where L is the fault length, we capture the same characteristics observed by *Okal and Synolakis* [2004] (see Figure 1). The rest of the parameters on equation (2) will be described in detail in the next section.

2.1. The Runup Distribution Along the Coastline: 2+1 D Problem

Modeling of runup distribution requires the use of the finiteness and size of a seismic source: thus, the strategy of this calculation is based on an analytic solution (equation (2)), which solves the 2+1 D runup problem for an incoming solitary-type wave in a sloping beach model inside a linear regime. It has been shown that solutions from linear theory can perform well enough in comparison to nonlinear theory [*Synolakis*, 1991]. *Melgar and*

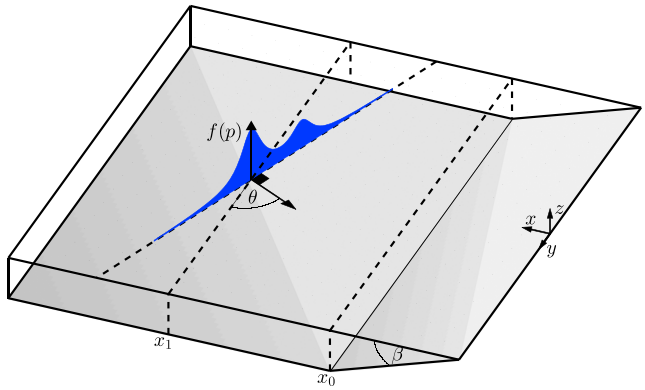

Figure 2. Sketch of the initial incoming wave for the particular solution analyzed in the 2+1 D case, showing the decay function, $f(p)$, along the transverse direction. The y direction represents the North. figure from *Fuentes et al.* [2013].

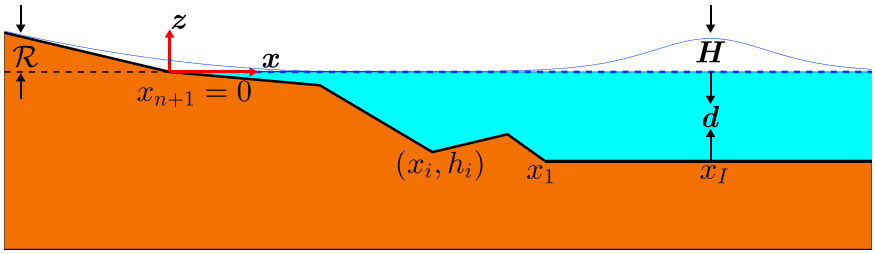

Figure 3. Sketch of the 1+1 D model. Figure from *Fuentes et al.* [2015].

Bock [2013] performed tests to verify the linearity assumption, proving that nonlinearity exists, but it is small compared to the maximum amplitude recorded on tsunami gauges. This just confirms that linear theory can accurately predict tsunami runup as a first-order approximation.

First, some parameters must be defined (Figure 2):

H is the maximum height of the initial wave; d is the mean ocean depth; β is the fore-arc wedge angle, θ is the incident angle of the incoming wave, and $f(p)$ is a function that represents the decay of the wave along the transverse direction. Thus, to run this model, the construction of the initial wave and a sloping beach approximation for the specific zone are needed.

For the initial wave, an FFM was used to account for the complexity of the seismic source. The static seafloor deformation is computed with Okada's formulas [*Okada*, 1985], and a decay function $f(p)$ is calculated for any given initial profile. To determine $f(p)$ from the location of the maximum initial wave (H), we extract a cross section in the fault strike direction. The resulting curve is normalized and made positive in order to scale maximum height along the whole rupture zone. Also, by taking the maximum value of the vertical deformation, we define H. The incidence angle of the tsunami raypath can be retrieved from the strike angle and the coastline orientation; however, in a worst case scenario when either the strike, fault plane, or orientation of the coast is not known, one always can start by setting $\theta = 90°$.

For the sloping beach, a bathymetry profile is extracted from GEBCO bathymetry (http://www.gebco.net/). In this way, one can easily retrieve the average ocean depth d and the fore-arc wedge angle β, which in most cases varies from 1° to 2° [*Rosenau et al.*, 2010].

With all the parameters defined, we can produce an analytic runup distribution using equation (2) in a few seconds, after the FFM is obtained.

In this study we exclude strike-slip tsunamigenic faults for two reasons: first, such earthquakes are generally located at ridges or in the middle of the ocean, which is not considered near field in this case; and second, strike-slip faults do not produce large amplitudes, because their radiation pattern is too weak [*Ward*, 1980].

2.2. The Runup in a Piecewise Linear Bathymetry: 1+1-D Problem

In our second approach the runup is estimated in a piecewise linear bathymetry [*Kânoğlu and Synolakis*, 1998; *Fuentes et al.*, 2015].

For this approach it is also necessary to model the initial wave and bathymetry. Because of the complexity of the problem, the analytic solution is available only for 1+1 D; thus, we trade off complexity in the source with complexity in bathymetry.

For this model, the following parameters are needed: H, the initial wave height (related to the seismic source) and the piecewise linear bathymetry approximation (Figure 3).

Being a 1+1 D problem, the best way to represent an average initial wave height, is by using a uniform slip distribution, which averages the amount of slip over the fault plane. Then, H can be obtained as the maximum vertical displacement transferred from the bottom of the ocean to the sea surface in a passive tsunami generation.

Similar to the 2+1 D case, we take the transect of the bathymetry, but here we approximate the profile shape with a piecewise linear function obtained with a least squares algorithm.

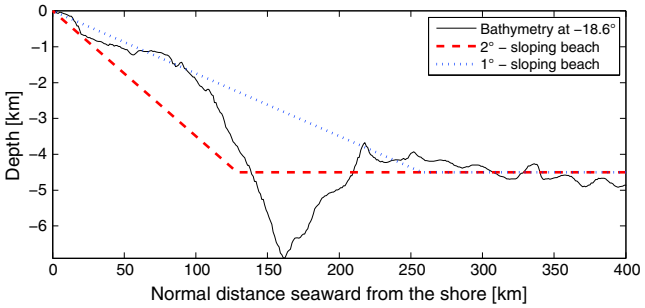

Figure 4. Example of the model setting in northern Chile.

When the whole set of parameters is retrieved, the runup can be estimated by

$$\mathcal{R} = 2.831H\left(\frac{H}{d}\right)^{\frac{1}{4}}\left(1+\frac{H}{d}\right)^{\frac{1}{4}}|b_{n+1}|^{-\frac{1}{2}} \tag{3}$$

where b_{n+1} is the slope of the segment closest to the shore, hereinafter *the last slope*.

For the M_w 7.7 Nicaragua earthquake, we chose an *N* wave as described by *Tadepalli and Synolakis* [1996], because the subsidence is restricted to the region between the trench and the coast.

2.3. Comments About Each Method

Using each formulation (equations (2) and (3)), a mathematical expression for the runup including the seismic source effect can be rewritten. Since this is an analytical solution, the calculation can be done in a few seconds.

Bathymetry available online (for instance, GEBCO) is high enough resolution to construct the models presented in this work (Figure 4). A remarkable result is that by using linear theory and knowing the parameters of the source, it is possible to obtain accurate estimation of runup using either formula.

It has been shown that the runup in a multisloping beach is only dependent on the bathymetric slope closest to the beach. For each earthquake the parameters are set to include the bathymetry along every subduction zone. After that the runup is calculated from both approximations: the theoretical solution on a simple bathymetry model and the multisloping approach [*Kânoğlu and Synolakis*, 1998; *Fuentes et al.*, 2015].

In this work the solitary wave (a wave that compensates for nonlinearity and dispersion) is used, because its mathematical treatment is simple and well known. From the early warning perspective, this method reduces response time in an emergency.

Our model describes the effects produced by the first incoming wave (linear theory) to the coast with a simple slope. Therefore, the maximum observed runup and the maximum theoretical runup show some differences, because the maximum observed runup may be the result of later arriving waves; also, fines-scale bathymetry not represented in our model influence these discrepancies. Furthermore, the 2+1 D model does not include refraction, loss of energy, bottom friction, wave breaking, resonance, or any sort of nonlinear perturbation.

For the 2+1 D model, it is difficult to approximate a complex bathymetry with only one slope and a mean depth. Therefore, two extreme slope angles are taken (1° and 2°) for the sloping beach model, and a mean depth, that corresponds to the open-ocean depth for each earthquake in this study is used. The idea is to explore the best and worst case scenarios with the maximum and minimum slopes, respectively (i.e., minimum and maximum runups).

From the multisloping (1+1 D) beach, given any moment tensor, we assume fault dimensions from *Blaser et al.* [2010] with uniform slip, then we estimate the maximum runup. Because the equation is solved in one dimension only, we calculate Okada's deformation and take a slice of the initial wave profile, and then use formula (3).

We do not consider tsunamis in islands, bays, estuaries, etc, in these approximations. We estimate runup in well-defined subduction zones only, represented by the idealized situation of a line where the source is inside the coastline; i.e., the fault plane is not larger than the coast line. This method does not work for tsunamis at complex areas, such as the tsunami of 1956 in Amorgos, Greece [*Okal et al.*, 2009].

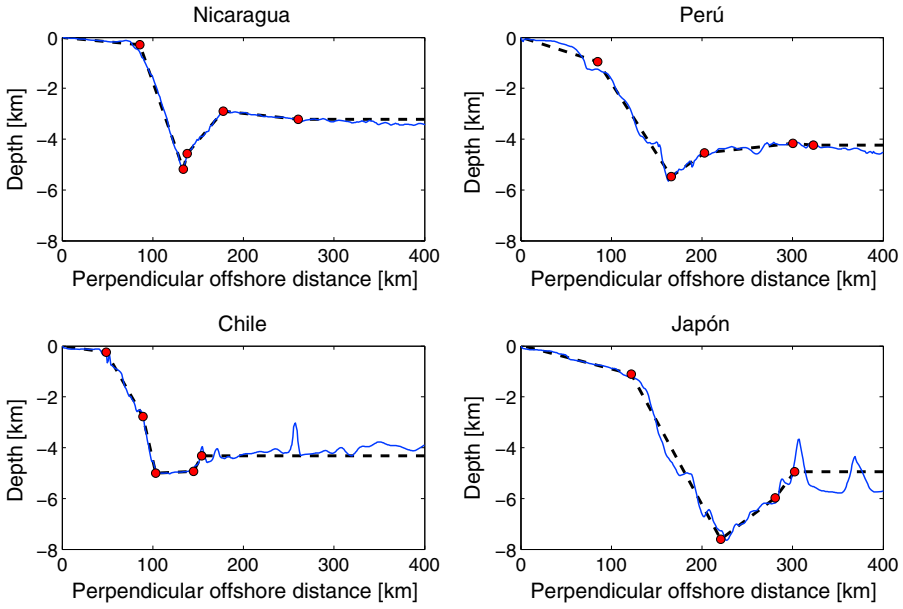

Figure 5. The 1+1 D bathymetry setting for some coast-trench profiles.

3. Results

The 2+1 D method gives a more accurate approximation than the approach proposed by *Okal and Synolakis* [2004]. This is because we include complexity from the finite fault model, and we extend the sloping beach model in the *y* direction along the trench. As previously discussed, runup can be underestimated up to 6 times under the assumption of uniform slip at the source. Incorporating slip complexity accounts for variability in the runup calculation [*Geist*, 2002; *Mueller et al.*, 2015; *Ruiz et al.*, 2015].

The 1+1 D method can accurately estimate maximum runup from the CMT alone. It is most appropriate when bathymetry contains abrupt slope changes, since runup is dependent on the last slope. For a fixed size of a large earthquake, subduction zones like Nicaragua, Southern Chile, Perú, Japan, etc., are prone to produce larger runup than other subduction zones from the last slope point of view. This generally results from the fact that the last slope is very smooth, for more than 50 km in some of these cases (Figure 5).

To retrieve the FFM for each earthquake for the 2+1 D approach, the algorithm proposed by *Ji et al.* [2002] was used. We choose this method because it has been proven to be reliable and robust for operational purposes at the United States Geological Survey (USGS) [e.g., *Hayes*, 2011; *Hayes et al.*, 2014]. The CMT parameters were retrieved from *W* phase inversions found at www.usgs.gov [*Duputel et al.*, 2012]. To retrieve *L* and *W*,

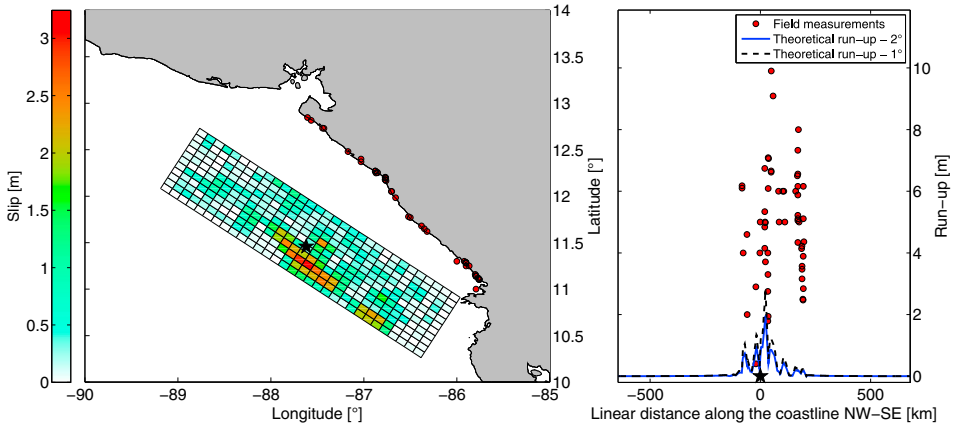

Figure 6. The 1992 Nicaragua earthquake finite fault inversion ($\mu = 3 \times 10^{10}$ N/m^2) and runup.

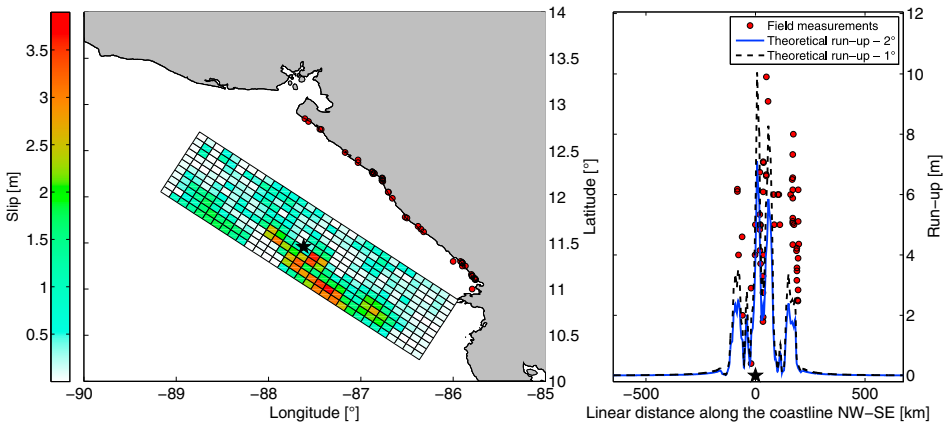

Figure 7. The 1992 Nicaragua earthquake finite fault inversion ($\mu = 1 \times 10^{10}$ N/m^2) and runup.

the scaling laws was taken from *Blaser et al.* [2010]: $\log(L) = -2.81 + 0.62M_w$ and $\log(W) = -1.79 + 0.45M_w$, assuming a shear modulus was 30 GPa except for the Nicaragua earthquake with a value of 10 GPa.

It is important to clarify that both FFM and W-phase algorithms operate in real time at the NEIC predominantly for teleseismic distances (though W-phase solutions are often published using regional stations for large earthquakes). Here we wish to show how powerful it would be to have both solutions available in real time using near-field data.

3.1. Earthquake Tested

We select several events to test these methods. Each case study was chosen because of their well-defined tectonic setting and because they have been broadly studied in terms of the seismic source properties and their corresponding tsunamis.

3.1.1. The 1992 M_w 7.7 Nicaragua Tsunami-Earthquake

This earthquake has been extensively studied. *Kikuchi and Kanamori* [1995] proposed a source model from seismic data, while *Satake* [1994] proposed a model from observed runups and tide gauge records. Each produces different results. The first showed an average slip of 1.3 m and the second, 3 m. Due to this discrepancy, we consider both approaches.

The earthquake and tsunami have interesting features: The source is a typical tsunami-earthquake [*Kanamori and Kikuchi*, 1992; *Kikuchi and Kanamori*, 1995], and the bathymetry shows a gentle slope of 0.0027 in the closest segment to the shore (Figure 5). This bathymetric feature leads to higher runup than other subduction zones.

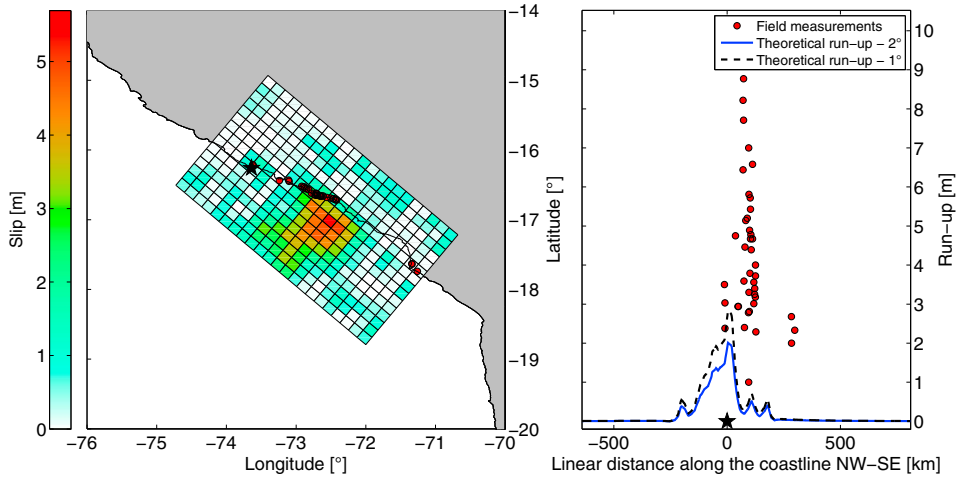

Figure 8. The 2001 Perú earthquake finite fault inversion and runup.

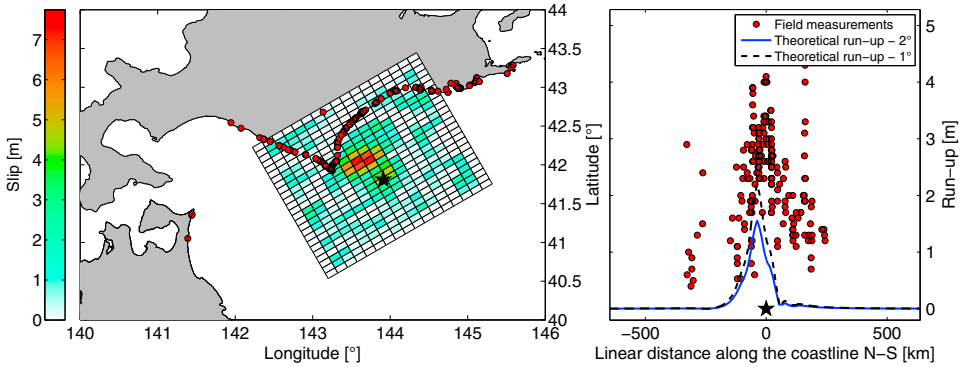

Figure 9. The 2003 Tokachi-Oki earthquake finite fault inversion and runup.

To calculate the 2+1 D analytical runup, first, we perform an inversion based on the velocity model proposed by *Kikuchi and Kanamori* [1995]; however, this model does not predict the runup as we expected (Figure 6).

From the tsunami point of view, the abnormally observed runup heights, discrepancies in the arrival times of waves in mareographs and the observed wave amplitudes in the ocean, could be retrieved from a source of $L = 250$ km, $W = 40$ km, $d = 3$ m, and a low shear modulus of 10 GPa [*Satake*, 1994, 1995; *Ihmlé*, 1996; *Piatanesi et al.*, 1996]. We perform an inversion using a velocity model proposed by *Sallarés et al.* [2013] obtaining a better fit with the observed runup data (Figure 7). The 2+1 D model shows a maximum runup of 6.8 and 9.6 m with both slopes (1° versus 2°).

For the multisloping CMT model, we obtain 6.7 m, considering a solitary wave. However, because the deformation is closer to the trench, the subsidence is located between the trench and the coastline. This means that the initial condition is suitable for a leading-depression N-shaped wave [*Tadepalli and Synolakis*, 1996]. Using this type-wave, we obtain 9.1 m.

3.1.2. The 2001 M_w 8.4 Perú Earthquake

The 2001 Perú earthquake produced a tsunami with a maximum runup of 8.2 m [*Okal et al.*, 2002] and according to our FFM a peak slip of 5.5 m (Figure 8). There are two runup measurements that are considered splash points [*Okal et al.*, 2002] and removed from the data. The multisloping approach fits well with the maximum observed runup; 8 and 8.2 m, respectively. However, the 2+1 D approach does not show good agreement with the data.

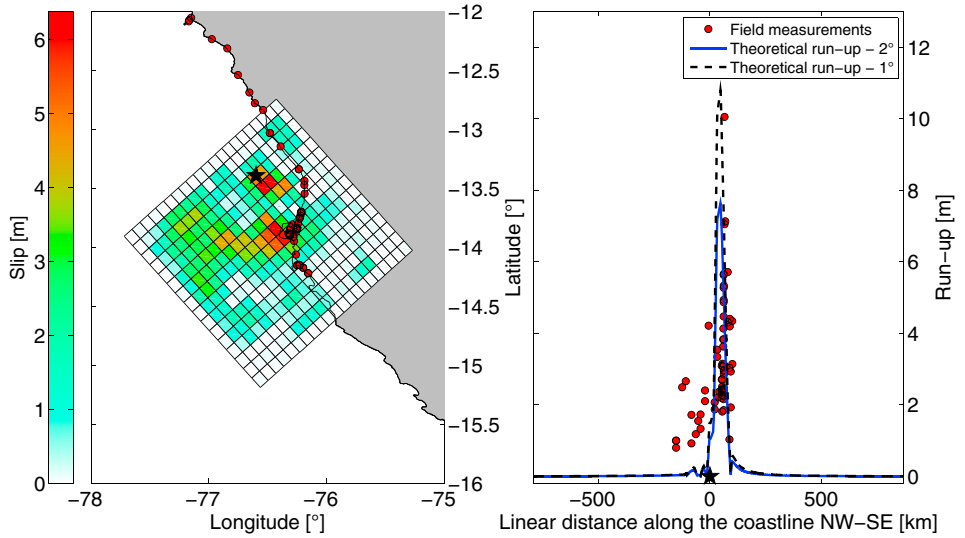

Figure 10. The 2007 Perú earthquake finite fault inversion and runup.

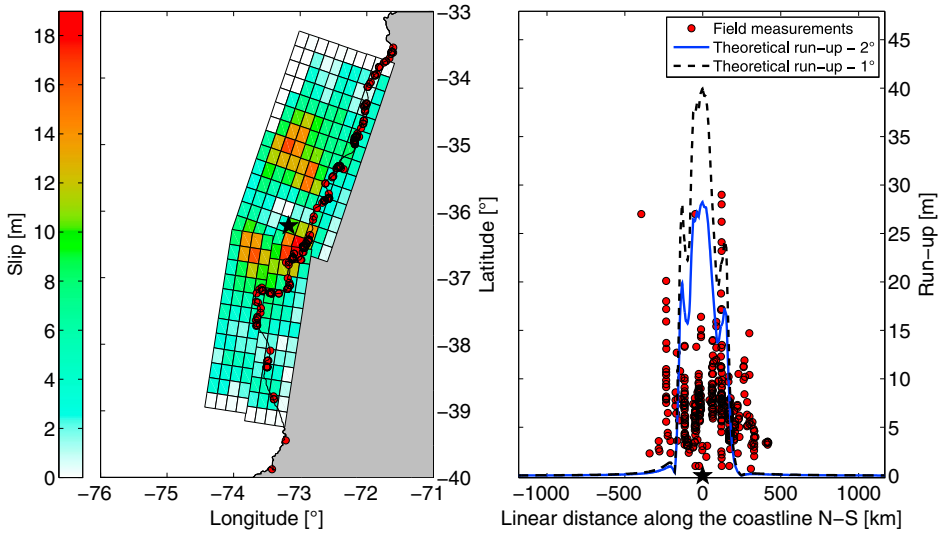

Figure 11. The 2010 Maule earthquake finite fault inversion and runup.

3.1.3. The 2003 M_w 8.2 Tokachi-Oki Earthquake

In this case the rupture is mainly concentrated in the lower portion of the subduction interface. The maximum slip from our finite fault inversion is 7.2 m (Figure 9). It generated a maximum runup of 4.4 m [*Tanioka et al.*, 2004]. Our 2+1 D tsunami solution does not reach the maximum runup, but the 1+1 D model using the CMT shows a runup of 6 m, more accurate than the 2+1 D model.

3.1.4. The 2007 M_w 8.2 Pisco Earthquake

The 2007 Pisco earthquake broke the middle portion of the subduction interface concentrating on the slip patch from 30 to 40 km depth. Our FFM implies a peak slip of 6.3 m. The peak runup was 10.1 m. The runup in the near field was measured from 12°S to 14.5°S, with a maximum runup of 10.1 m and 7.1 m, both in Playa Yumaque [*Fritz et al.*, 2007]. These points were extracted from the runup data because they are associated with a very rugged coastline. Nevertheless, we obtain agreement with the models (Figure 10).

The 2+1 D analytical and the 1+1 D multisloping models predicted 5.4 m and 9.2 m from the FFM and the CMT, respectively.

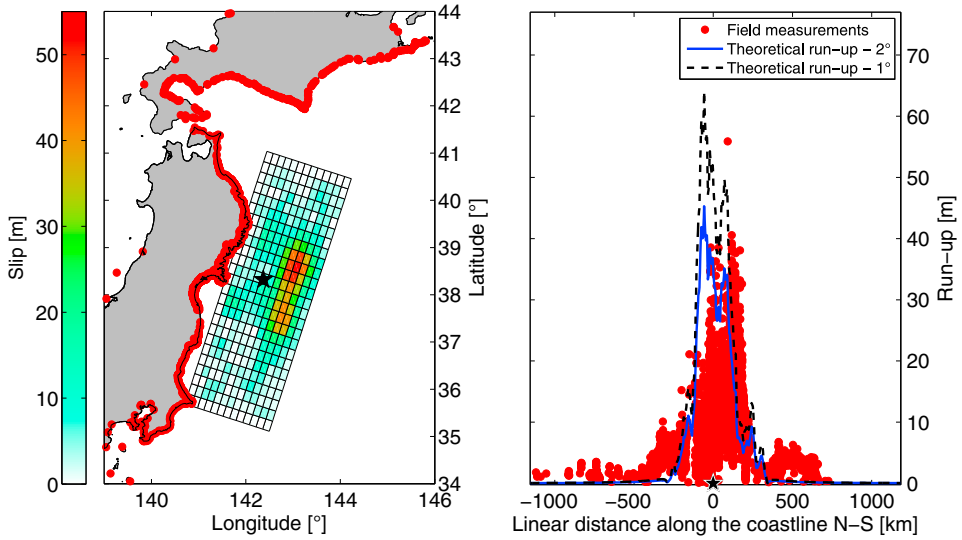

Figure 12. The 2011 Tohoku earthquake finite fault inversion and runup.

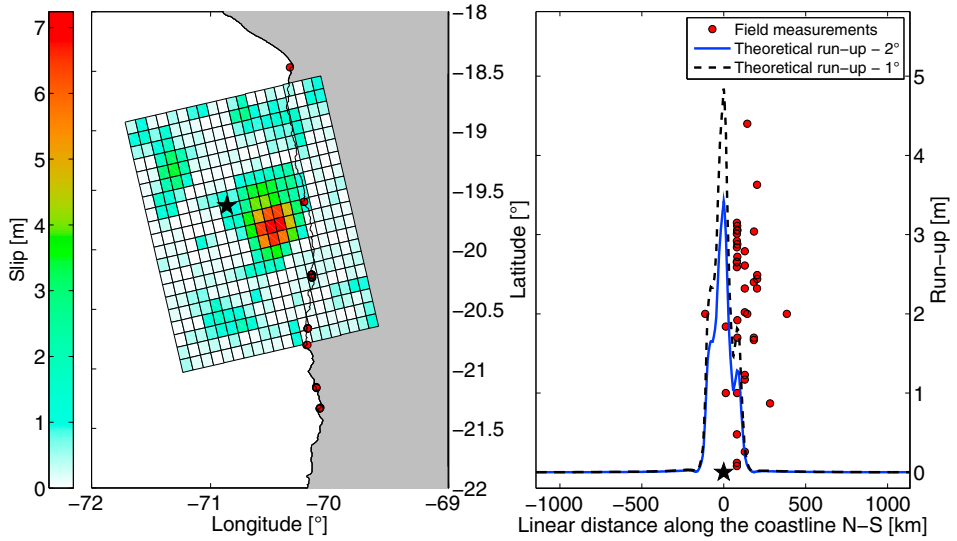

Figure 13. The 2014 Iquique earthquake finite fault inversion and runup.

3.1.5. The 2010 M_w 8.8 Maule Earthquake

The FFM proposed by *Hayes et al.* [2013] shows a peak slip of 18 m, while the maximum runup reached 29 m [*Fritz et al.*, 2011]; those authors show that larger runup measurements extend from ≈34°S to 39°S (Figure 11). This event produced a far-field tsunami. The analytical model predicts 31 – 40 m peak runup, showing agreement with the larger slip patches at the source. The multisloping CMT model also gives a good approximation of the peak runup, 31 m.

The bathymetry in this area is similar to the profile from Nicaragua. The closest segment to the shore compared to the next distant segment exhibits an abrupt change in the slope from gentle to steeper (Figure 5), which increases the possibility of larger runup.

3.1.6. The 2011 M_w 9.1 Tohoku Earthquake

The Tohoku-Oki earthquake, M_w 9.1, broke the upper part of the subduction zone [*Hayes*, 2011] reaching the trench and showing bathymetric changes produced by the earthquake [*Fujiwara et al.*, 2011]. This event also produced a far-field tsunami. The FFM shows a peak slip of 40 m [*Hayes*, 2011]. The peak-observed runup reached 40 m [*Mori et al.*, 2011]. The analytical model predicts runups of 45 and 64 m, for 2° and 1°, respectively. The runup extended from Chiba to Hokkaido [*Mori et al.*, 2011]. The southern (≈34° – 35°N) and the northern (≈41° – 43°N) part of the coast is less affected by the runup because the energy is concentrated in the middle portion of the rupture. The peak runup coincides with the major energy released from the earthquake (Figure 12). The CMT multisloping method predicts 41 m runup again in agreement with the observed maximum runup.

3.1.7. The 2014 M_w 8.2 Iquique Earthquake

The Iquique earthquake broke the middle part of the subduction interface, with a maximum slip of 7.2 m, located at 40 m depth [*Hayes et al.*, 2014]. It produced a tsunami with a peak runup of 4.4 m. The 2+1 D model predicts runups of 3.4 m and 4.8 m for each slope angle and the CMT 1+1 D model predicts a runup

Table 1. Source Parameters For Past Earthquakes in the Peruvian Coast[a]

Event	M_w	L	W	Depth	$\overline{\Delta u}$	Dip	Strike	d	b_{n+1}	$\mathcal{R}_{1+1D}$	$\mathcal{R}_{Sim}$
3 Oct 1974 (a)	8.1	150	40	22	5	17	330	4.2	0.0056	8.9	3.2
3 Oct 1974 (b)	8.1	250	40	22	3	17	330	4.2	0.0056	4.2	3
13 Aug 1868 (a)	9.2	600	150	20	15	20	305	4.5	0.0218	26	33
13 Aug 1868 (b)	9.3	900	150	20	15	20	305	4.5	0.0218	26	28

[a]Moment magnitude M_w, length L (km), width W (km), depth (km), average slip $\overline{\Delta u}$ (m), and mechanism are taken from *Okal et al.* [2006]. Rake is 90° for each earthquake. Mean seafloor depth d (km) and last slope are estimated as described in section 2 for the 1+1 D CMT approach, $\mathcal{R}_{1+1D}$ (m) is estimated runup, and $\mathcal{R}_{Sim}$ (m) is simulated runup from *Okal et al.* [2006].

Table 2. Summary for Tsunami Runup Scaling Laws and Results From the Analytical Solutions for Each Earthquake in This Study[a]

Event	M_w	$\mathcal{R}_A$	Δu_{max}	$\mathcal{R}_P$	$\mathcal{R}_{Obs}$	$\mathcal{R}_{2+1D}$
Nicaragua 1992	7.7	3.6	4.7	9.4	9.9	6.8–9.6
Perú 2001	8.4	7.9	5.5	11	8.2	2–2.8
Tokachi-oki 2003	8.2	6	7.5	15	4.4	1.6–2.2
Pisco 2007	8.2	6.1	6.3	12.6	7.1	3.9–4.5
Maule 2010	8.8	13.2	18.5	34	29	28.4–40.2
Tohoku 2011	9.1	17.8	55	110	40.6	45.4–64.2
Iquique 2014	8.2	6.2	7.2	14.4	4.4	3.4–4.8

[a]Abe Tadepalli and Synolakis The 1992 M_w 7.7 tsunami-earthquake Nicaragua is modeled as shown in Figure 7. M_w is moment magnitude, Abe's scale runup $\mathcal{R}_A$ (m) [*Abe*, 1995], maximum slip Δu_{max} (m), maximum Plafker runup $\mathcal{R}_P$, observed runup $\mathcal{R}_{Obs}$ (m), estimated 2+1 D runup $\mathcal{R}_{2+1D}$ (m) with 2° and 1°, respectively. For the 1992 Nicaragua earthquake if an *N* wave [*Tadepalli and Synolakis*, 1996] is chosen, runup is 9.1 m.

of 4.1 m (Figure 13). As expected, the deeper location of the maximum slip dictates the relatively small runup compared to other earthquakes with similar or lower magnitude shown in this study.

3.2. Past Earthquakes

In order to compare the 1+1 D CMT model with full numerical calculations, the study of *Okal et al.* [2006] is used. This study shows uniform slip distributions and their correspond predicted runup. We compared the runup obtained with the 1+1 D CMT method and the runup presented in this study. Four different sources from two past earthquakes are chosen: The 1868 Africa earthquake and the 1974 Lima earthquake. The results are presented in Table 1.

The results are dependant on the last slope and the sources chosen. The 1974 earthquake shows a numerical runup closer to the analytical runup with a longer source in the along-strike direction (Table 1). The shorter source concentrates more slip, and therefore, the runup is larger in this case. For the 1868 earthquake, there is no change in the runup from the 1+1 D CMT method when the source is lengthened from 600 km to 900 km, because the uniform slip is the same in both sources; however, the maximum runup from both numerical calculations is close to that obtained from the analytical method.

3.3. Discussion

In general, both models are sensitive to the bathymetric slope, which does not scale linearly. This is attributed to the singularity at the origin of the function $\cot(\cdot)$, used to derive $\mathcal{R}_0$. Nonetheless, the 2+1 D approach is less sensitive to bathymetry than the 1+1 D approach. This is due to the fact that bathymetry close to the shore becomes gentler, as opposed to using one average slope to represent the overall bathymetry. The 1+1 D approach is also very dependent on the chosen scaling law. It is important to choose a scaling law [*Wells and Coppersmith*, 1994; *Blaser et al.*, 2010; *Strasser et al.*, 2010; *Murotani et al.*, 2013] according to the type of earthquake that we are trying to model. For tsunami early warning purposes, the scaling law used to estimate the maximum runup should always be that which implies larger slip, because it will always generate larger deformation at the ocean bottom.

For each earthquake, finite fault models derived using different modeling approaches need to be tested. This will help us to understand how sensitive our model is to different inputs and what the role of bathymetry is in each case, since the scaling of runup is related to local bathymetric effects, to the FFM, or to a combination of both. Furthermore, certain bathymetries could generate resonance associated with trapped waves between the accretionary wedge and the continental shelf [*Yamazaki and Cheung*, 2011]. This could amplify runup after the first incoming wave; thus, the waves coming after the first arrival may generate higher runup. In our model no such effects are included and underestimation or overestimation in some cases is therefore expected.

Plafker [1997] pointed out that, if there are no abrupt changes in topography along the coastline, the amplitude of maximum runup is of the order of the maximum slip at the fault and it cannot be more than twice the peak slip at the source. *Abe* [1995] showed that runup scales exponentially with the moment magnitude and *Rosenau et al.* [2010] linearly with the slip at the source. The proposed methods produce similar results to these previous studies indicated here, making, implying these rules of thumb are robust for tsunami early warning purposes (Tables 2 and 3).

Table 3. Source Paramenters for 1+1 D CMT Method[a]

Event	M_w	μ	L	W	Depth	$\overline{\Delta u}$	Strike	Dip	Rake	d	b_{n+1}	$\mathcal{R}_{1+1D}$	$\mathcal{R}_{Obs}$
Nicaragua 1992	7.7	10	250	40	12	3	303	12	91	2.9	0.0027	9.1 (*)	9.9
Perú 2001	8.4	30	250	98	24	6.8	310	18	63	4.2	0.0176	8.1	8.2
Tokachi-oki 2003	8.2	30	188	79	24	5	250	11	132	5.2	0.0102	6	4.4
Pisco 2007	8.2	30	188	79	34	5	321	28	63	4.2	0.0053	9.2	7.1
Maule 2010	8.8	30	443	148	36	10	16	14	104	3.9	0.0034	32	29
Tohoku 2011	9.1	30	678	202	12	16	193	14	81	5.8	0.0068	40	40.6
Iquique 2014	8.2	30	188	79	26	5.2	358	12	107	4.5	0.0223	4.5	4.4

[a]Moment magnitude M_w, μ (GPa), length L (km), width W (km), average slip $\overline{\Delta u}$ (m), and mechanisms are taken from NEIC COMCAT. Mean seafloor depth d (km) and last slope are estimated as described in section 2 for the 1+1 D CMT approach. $\mathcal{R}_{1+1D}$ (m) is estimated runup and $\mathcal{R}_{Obs}$ (m) is the observed runup.

We note that we are sacrificing accuracy for speed in these methods. We performed a full numerical calculation using the software NEOWAVE (Nonhydrostatic Evolution of Ocean Wave) [*Yamazaki et al.*, 2009, 2011] for the M_w 8.8 Maule earthquake using a grid of 30 s and 1024 × 2120 points, to model 6 h of tsunami. This took us 20 h on a machine with 16 cores, an Intel Xeon 2.7 GHz processor and 128 GB RAM. For subduction zones, e.g., like Chile, where the trench is closer to the coast. It is important to have a rapid, first-order solution of runup like the one that we propose.

Horizontal advection in the $f(p)$ function can be included, but only in the static case. This depends on the chosen linearization of bathymetry and its representation in segments described above. This could be a subject of a future work, testing the sensitivity of the method to how the deformation is calculated, and what is the impact of horizontal deformation for each earthquake is in its corresponding subduction zone.

GPS signal, do not clip in the near field. Therefore, recent advances made in real-time GPS data collection and processing will make it possible to retrieve the CMT and any FFM within the first 5 min after any large earthquake that occurs close to such a network [*Blewitt et al.*, 2009; *Crowell et al.*, 2012; *Ohta et al.*, 2012; *Melgar and Bock*, 2013; *Grapenthin et al.*, 2014], and consequently its runup estimation from these two models can be derived very quickly.

Finally, while it is possible that inundation could be estimated from runup estimates provided by these methods, there are many of complexities in the coastal zone that influence inundation (frontal dunes, vegetation, etc.)., which are not considered here.

4. Conclusions

In this work a new methodology to produce a first-order approximation of runup distribution along the coastline is proposed, which has the potential to be applied in tsunami early warning systems.

In the CMT multisloping model, bathymetry makes a considerable difference to the predicted value of runup. Given any initial wave, it is possible to determine the zones that are prone to having larger runup than others because of the bathymetry. To solve this problem, we pass from 2+1 D dimensions to 1+1 D dimensions. Nevertheless we still can reconstruct the observed runup well enough if the strike is the same along the trench and the coastline. For future studies, the 2+1 D multisloping problem should be explored in more detail. For a specific zone, when all the required analytical conditions are satisfied; i.e., as a well constrained subduction environment, a bathymetry that can be approximated by a slope or multislope beach model, a straight coast, and a source which is not larger than the coast [*Fuentes et al.*, 2013, 2015], then a well-constrained FFM should best explain the observed runup heights.

The Nicaragua 1992 earthquake has a special behavior from two points of view: the complex source of this event (including a very low shear modulus, μ) and the extended rupture time and its consequent large slip. The bathymetry in this area, having a gentle last slope of 0.0027 (0.015°) obviously increases the runup height. Only a small decrease in the slope increases the initial wave amplitude (equation (3)). For the specific location of El Transito (runup: 9.9 m), as *Synolakis and Kong* [2006] pointed out in their study for the Indian Ocean tsunami, the presence of an opening reef can increase the runup height.

The 2+1 D method works well in zones with a strongly constrained and defined tectonic (subduction) setting that could possibly generate large earthquakes. It was mainly built to have a rapid first-order approximation of the tsunami runup as soon as an FFM is available. This is a tool for emergency response; the main goal is not to be exact but to give an approximated runup through an analytical solution as soon as we have any FFM.

Even if tsunami models include variable slip from the source, for modeling them numerically in real time, a few hours are needed. Therefore, they are not useful for early warning purposes. The fact that both methods discussed are derived from analytic equations make them faster than any other numerical model and do not require high-performance computers to obtain an estimation of runup.

Acknowledgments
This work was supported by FONDECYT1130636 and Programa Riesgo Sísmico (AIN U. de Chile). The data used for finite fault models and centroid moment tensor solutions are public and were obtained from the United States Geological Survey (http://www.usgs.gov). The bathymetric data are public and were obtained from the General Bathymetry Charts of the Ocean (http://www.gebco.net). The runup measurements were obtained from the National Oceanic and Atmospheric Administration (http://www.ngdc.noaa.gov). We are grateful to Eric Geist and two anonymous reviewers who made interesting suggestions and comments to improve this paper. Any use of trade, firm, or product names is for descriptive purposes only and does not imply endorsement by the U.S. government.

References

Abe, K. (1995), Estimate of tsunami runup heights from earthquake magnitudes, in *Tsunami: Progress in Prediction, Disaster Prevention and Warning*, edited by Y. Tsuchiya and N. Shuto, pp. 21–35, Springer, Netherlands.

Andrews, D. (1980), A stochastic fault model: 1. Static case, *J. Geophys. Res.*, *85*(B7), 3867–3877.

Andrews, D. (1981), A stochastic fault model: 2. Time-dependent case, *J. Geophys. Res.*, *86*(B11), 10,821–10,834.

Bernard, P., A. Herrero, and C. Berge (1996), Modeling directivity of heterogeneous earthquake ruptures, *Bull. Seismol. Soc. Am.*, *86*(4), 1149–1160.

Blaser, L., F. Krüger, M. Ohrnberger, and F. Scherbaum (2010), Scaling relations of earthquake source parameter estimates with special focus on subduction environment, *Bull. Seismol. Soc. Am.*, *100*, 2914–2926.

Blewitt, G., W. Hammond, C. Kreemer, H.-P. Plag, S. Stein, and E. Okal (2009), GPS for real-time earthquake source determination and tsunami warning systems, *J. Geod.*, *83*(3–4), 335–343.

Borrero, J., S. Cho, J. Moore, H. Richardson, and C. Synolakis (2005), Could it happen here, *Am. Soc. Civil Eng.*, *75*(4), 54–65,133.

Crowell, B. W., Y. Bock, and D. Melgar (2012), Real-time inversion of GPS data for finite fault modeling and rapid hazard assessment, *Geophys. Res. Lett.*, *39*, L09305, doi:10.1029/2012GL051318.

Duputel, Z., L. Rivera, H. Kanamori, and G. Hayes (2012), W phase source inversion for moderate to large earthquakes (1990–2010), *Geophys. J. Int.*, *189*, 1125–1147.

Fritz, H., N. Kalligeris, J. Borrero, P. Broncano, and E. Ortega (2007), The 15 August 2007 Peru tsunami run-up observations and modeling, *Geophys. Res. Lett.*, *35*, L10604, doi:10.1029/2008GL033494.

Fritz, H., et al. (2011), Field survey of the 27 February 2010 Chile tsunami, *Pure Appl. Geophys.*, *168*(11), 1989–2010.

Fuentes, M., J. Ruiz, and A. Cisternas (2013), A theoretical model of tsunami run-up in Chile based on a simple bathymetry, *Geophys. J. Int.*, *196*(2), 986–995, doi:10.1093/gji/ggt426.

Fuentes, M., J. Ruiz, and S. Riquelme (2015), The run-up on a multilinear sloping beach model, *Geophys. J. Int.*, *201*(2), 915–928.

Fujiwara, T., S. Kodaira, T. No, Y. Kaiho, N. Takahashi, and Y. Kaneda (2011), The 2011 Tohoku-Oki earthquake: Displacement reaching the trench axis, *Science*, *334*(6060), 1240–1240.

Geist, E. (2002), Complex earthquake rupture and local tsunamis, *J. Geophys. Res.*, *107*(B5), ESE 2–1–ESE 2-15, doi:10.1029/2000JB000139.

Grapenthin, R., I. Johanson, and R. Allen (2014), Operational real-time GPS-enhanced earthquake early warning, *J. Geophys. Res. Solid Earth*, *119*, 7944–7965, doi:10.1002/2014JB011400.

Hayes, G. (2011), Rapid source characterization of the 2011 M_w 9.0 off the Pacific coast of Tohoku earthquake, *Earth Planets Space*, *63*, 529–534.

Hayes, G., E. Bergman, K. Johnson, H. M. Benz, L. Brown, and A. Meltzer (2013), Seismotectonic framework of the February 27, 2010 M_w 8.8 Maule, Chile earthquake sequence, *Geophys. J. Int.*, *195*, 1034–1051, doi:10.1093/gji/ggt238.

Hayes, G., M. Herman, W. Barnhart, K. Furlong, S. Riquelme, H. Benz, E. Bergman, S. Barrientos, P. Earle, and S. Samsonov (2014), Continuing megathrust earthquake potential in Northern Chile after the 2014 Iquique earthquake sequence, *Nature*, *512*, 295–298, doi:10.1038/nature13677.

Hearn, E. H., and R. Bürgmann (2005), The effect of elastic layering on inversions of GPS data for earthquake slip and stress changes, *Bull. Seismol. Soc. Am.*, *95*, 1637–1653.

Herrero, A., and P. Bernard (1994), A kinematic self-similar rupture process for earthquakes, *Bull. Seismol. Soc. Am.*, *84*(4), 1216–1228.

Hoechner, A., M. Ge, A. Babeyko, and S. Sobolev (2013), Instant tsunami early warning based on real-time GPS-Tohoku 2011 case study, *Nat. Hazards Earth Syst. Sci.*, *13*(5), 1285–1292.

Ihmlé, P. (1996), Monte Carlo slip inversion in the frequency domain: Application to the 1992 Nicaragua slow earthquake, *Geophys. Res. Lett.*, *23*(9), 913–916.

Ji, C., D. Wald, and D. Helmberger (2002), Source description of the 1999 Hector Mine, California, earthquake, Part I: Wavelet domain inversion theory and resolution analysis, *Bull. Seismol. Soc. Am.*, *92*, 1192–1207.

Kanamori, H., and M. Kikuchi (1992), The 1992 Nicaragua earthquake: A slow tsunami earthquake associated with subducted sediments, *Nature*, *361*, 714–716.

Kanamori, H., and L. Rivera (2008), Source inversion of W phase: Speeding up seismic tsunami warning, *Geophys. J. Int.*, *175*(1), 222–238.

Kânoğlu, U., and C. Synolakis (1998), Long wave run-up on piecewise linear topographies, *J. Fluid Mech.*, *374*, 1–28.

Kikuchi, M., and H. Kanamori (1995), Source characteristics of the 1992 Nicaragua tsunami earthquake inferred from teleseismic body waves, *Pure Appl. Geophys.*, *144*(3–4), 441–453.

Lomax, A., and A. Michelini (2009), Tsunami early warning using earthquake rupture duration, *Geophys. Res. Lett.*, *36*, L09306, doi:10.1029/2009GL037223.

Lomax, A., and A. Michelini (2011), Tsunami early warning using earthquake rupture duration and P wave dominant period: The importance of length and depth of faulting, *Geophys. J. Int.*, *185*(1), 283–291.

Ma, S. (2012), A self-consistent mechanism for slow dynamic deformation and tsunami generation for earthquakes in the shallow subduction zone, *Geophys. Res. Lett.*, *39*, L11310, doi:10.1029/2012GL051854.

Melgar, D., and Y. Bock (2013), Near-field tsunami models with rapid earthquake source inversions from land- and ocean-based observations: The potential for forecast and warning, *J. Geophys. Res. Solid Earth*, *118*, 5939–5955, doi:10.1002/2013JB010506.

Melgar, D., and Y. Bock (2015), Kinematic earthquake source inversion and tsunami runup prediction with regional geophysical data, *J. Geophys. Res. Solid Earth*, *120*, 3324–3349, doi:10.1002/2014JB011832.

Mori, N., T. Takahashi, T. Yasuda, and H. Yanawisawa (2011), Survey of 2011 Tohoku earthquake tsunami inundation and run-up, *Geophys. Res. Lett.*, *38*, L00G14, doi:10.1029/2011GL049210.
Mueller, C., W. Power, S. Fraser, and X. Wang (2015), Effects of rupture complexity on local tsunami inundation: Implications for probabilistic tsunami hazard assessment by example, *J. Geophys. Res. Solid Earth*, *120*, 488–502, doi:10.1002/2014JB011301.
Murotani, S., K. Satake, and Y. Fujii (2013), Scaling relations of seismic moment, rupture area, average slip, and asperity size for $M_w \sim 9$ subduction zone earthquakes, *Geophys. Res. Lett.*, *40*, 5070–5074, doi:10.1002/grl.50976.
Ohta, Y., et al. (2012), Quasi real-time fault model estimation for near-field tsunami forecasting based on RTK-GPS analysis: Application to the 2011 Tohoku-Oki Earthquake (M_w 9.0), *J. Geophys. Res.*, *117*, B02311, doi:10.1029/2011JB008750.
Okada, Y. (1985), Surface deformation due to shear and tensile faults in a half-space, *Bull. Seismol. Soc. Am.*, *75*, 1135–1154.
Okal, E., and C. Synolakis (2004), Source discriminants for near-field tsunamis, *Geophys. J. Int.*, *158*, 899–912.
Okal, E., et al. (2002), A field survey of the Camaná, Perú tsunami of June 23, 2001, *Seismol. Res. Lett.*, *73*, 904–917.
Okal, E., J. Borrero, and C. Synolakis (2006), Evaluation of Tsunami risk from regional earthquakes at Pisco, Peru, *Bull. Seismol. Soc. Am.*, *96*(5), 1634–1648.
Okal, E., C. Synolakis, B. Uslu, N. Kalligeris, and V. Voukouvalas (2009), The 1956 earthquake and tsunami in Amorgos, Greece, *Geophys. J. Int.*, *178*(3), 1533–1554.
Piatanesi, A., S. Tinti, and I. Gavagni (1996), The slip distribution of the 1992 Nicaragua earthquake from tsunami run-up data, *Geophys. Res. Lett.*, *23*(1), 37–40.
Plafker, G. (1997), Catastrophic tsunami generated by submarine slides and backarc thrusting during the 1992 earthquake on eastern Flores Island, Indonesia, *Geol. Soc. Am. Abstr. Programs*, *29*, 57.
Reymond, D., E. Okal, H. Hébert, and M. Bourdet (2012), Rapid forecast of tsunami wave heights from a database of pre-computed simulations, and application during the 2011 Tohoku tsunami in French Polynesia, *Geophys. Res. Lett.*, *39*, L11603, doi:10.1029/2012GL051640.
Rosenau, M., R. Nerlich, S. Brune, and O. Oncken (2010), Experimental insights into the scaling and variability of local tsunamis triggered by giant subduction megathrust earthquakes, *J. Geophys. Res.*, *115*, B09314, doi:10.1029/2009JB007100.
Ruiz, J., M. Fuentes, S. Riquelme, J. Campos, and A. Cisternas (2015), Numerical simulation of tsunami runup in northern Chile based on non-uniform k^{-2} slip distribution, *Nat. Hazards*,1–22, doi:10.1007/s11069-015-1901-9.
Sallarés, V., A. Meléndez, M. Prada, C. R. Ranero, K. McIntosh, and I. Grevemeyer (2013), Overriding plate structure of the Nicaragua convergent margin: Relationship to the seismogenic zone of the 1992 tsunami earthquake, *Geochem. Geophys. Geosyst.*, *14*, 3436–3461, doi:10.1002/ggge.20214.
Satake, K. (1994), Mechanism of the 1992 Nicaragua tsunami earthquake, *Geophys. Res. Lett.*, *21*, 2519–2522.
Satake, K. (1995), Linear and nonlinear computations of the 1992 Nicaragua earthquake tsunami, *Pure Appl. Geophys.*, *144*, 455–470.
Satake, K., J. Bourgeois, K. Abe, K. Abe, Y. Tsuji, F. Imamura, Y. Lio, H. Katao, E. Noguera, and F. Estrada (1993), Tsunami field survey of the 1992 Nicaragua earthquake, *Eos Trans. AGU*, *74*(13), 145–157.
Strasser, F. O., M. C. Arango, and J. J. Bommer (2010), Scaling of the source dimensions of interface and intraslab subduction-zone earthquakes with moment magnitude, *Seismol. Res. Lett.*, *81*(6), 941–950.
Synolakis, C. (1987), The runup of solitary waves, *J. Fluid Mech.*, *185*, 523–545.
Synolakis, C. (1991), Tsunami runup on steep slopes: How good linear theory really is, *Nat. Hazards*, *4*, 221–234.
Synolakis, C., and L. Kong (2006), Runup measurements of the December 2004 Indian Ocean Tsunami, *Earthquake Spectra*, *22*(S3), 67–91.
Tadepalli, S., and C. E. Synolakis (1996), Model for the leading waves of tsunamis, *Phys. Rev. Lett.*, *77*(10), 2141.
Tang, L., et al. (2012), Direct energy estimation of the 2011 Japan tsunami using deep-ocean pressure measurements, *J. Geophys. Res.*, *117*, C08008, doi:10.1029/2011JC007635.
Tanioka, Y., et al. (2004), Tsunami run-up heights of the 2003 Tokachi-oki earthquake, *Earth Planets Space*, *56*(3), 359–365.
Titov, V., C. Moore, D. Greenslade, C. Pattiaratchi, R. Badal, C. Synolakis, and U. Kânoğlu (2011), A new tool for inundation modeling: Community Modeling Interface for Tsunamis (ComMIT), *Pure Appl. Geophys.*, *168*(11), 2121–2131, doi:10.1007/s00024-011-0292-4.
Ward, S. (1980), Relationships of tsunami generation and an earthquake source, *J. Phys. Earth*, *28*(5), 441–474.
Ward, S. (2011), Tsunami, in *Encyclopedia of Solid Earth Geophysics*, edited by H. Gupta, pp. 1473–1493, Springer, Netherlands.
Wells, D., and K. Coppersmith (1994), New empirical relationships among magnitude, rupture length, rupture width, rupture area, and surface displacement, *Bull. Seismol. Soc. Am.*, *84*, 974–1002.
Yamazaki, Y., and K. F. Cheung (2011), Shelf resonance and impact of near-field tsunami generated by the 2010 Chile earthquake, *Geophys. Res. Lett.*, *38*, L12605, doi:10.1029/2011GL047508.
Yamazaki, Y., Z. Kowalik, and K. Cheung (2009), Depth-integrated, non-hydrostatic model for wave breaking and run-up, *Int. J. Numer. Methods Fluids*, *61*(5), 473–497.
Yamazaki, Y., K. Cheung, and Z. Kowalik (2011), Depth-integrated, non-hydrostatic model with grid nesting for tsunami generation, propagation, and run-up, *Int. J. Numer. Methods Fluids*, *67*(12), 2081–2107.